Active ferromagnetic shimming of the permanent magnet for magnetic resonance imaging scanner*

Tang Xin(唐 昕), Hong Li-Ming(洪礼明)‡, and Zu Dong-Lin(俎栋林)†

Institute of Heavy Ion Physics, Beijing Key Laboratory of Medical Physics and Engineering, School of Physics, Peking University, Beijing 100871, *China*

(Received 22 October 2009; revised manuscript received 21 November 2009)

This paper presents an approach of active ferromagnetic shimming for C-type permanent magnetic resonance imaging (MRI) magnet. It is designed to reduce inhomogeneity of magnetostatic field of C-type permanent magnet to meet the stringent requirement for MRI applications. An optimal configuration (locations and thicknesses) of active ferromagnetic pieces is generated through calculation according to the initial field map and the demanded final homogeneity specifications. This approach uses a minimisation technique which makes the sum of squared magnetic moment minimum to restrict the amount of the active ferromagnetic material used and the maximal thickness of pieces stacked at each hole location in the shimming boards. Simulation and experimental results verify that the method is valid and efficient.

Keywords: magnetic resonance imaging, active ferromagnetic shimming, permanent magnet, NdFeB pieces

PACC: 8760G, 8760I, 8760D, 4110D

1. Introduction

As well known there are two kinds of magnetic resonance imaging (MRI)[1−3] magnets: closed cylindrical superconductive (SC) magnet and open biplanar-pole permanent magnet such as the C-shaped one. The open space of the C-magnet helps the patient overcome any feelings of claustrophobia that may be experienced in a closed cylindrical magnet. Both the SC and permanent magnet must be shimmed to reduce the inhomogeneity of the magnetic field in the working magnetic field volume to within a predetermined specification, i.e. within a few or tens parts per million for use in medical diagnosis. However, to the permanent magnet due to approximation in the design as well as magnetising and fabricating tolerances, the homogeneity of main magnet field is often far away from the acceptable level. Therefore, shimming technology is of major importance in the design and manufacture of permanent MRI magnet. Many papers[4−8] and patents[9−11] published focus on passive steel shimming of the SC magnet. As for active coil shimming of the SC magnet, likewise there are many papers[12−14] published. The recent target field method[15−20] has been used for active shimming of the SC magnet.

Conventional electromagnetic shimming follows the approach based on representing the field as a spherical harmonics series: $B_z(r,\theta,\phi) = \sum_{n=0}^{\infty}\sum_{m=0}^{n} r^n P_n^m(\cos\theta)(A_n^m\cos(m\phi)+B_n^m\sin(m\phi))$. Amplitudes of harmonic components (A_n^m, B_n^m) are calculated from the magnetic field measured in or around imaging region. To the MRI permanent magnet[21−23] including spaced-apart first and second pole faces, a common active current shimming technique is the use of biplanar correction coils.[24,25] Biplanar coils consist of windings placed on parallel planes, and the magnetic field of interest is created in the space between them. These coils are designed to produce corresponding spherical harmonics[12] and have the merit of not interfering with each other. Generally speaking, active current shimming is used for corrections after a patient's access. Recent progress is that Forbes *et al.*[26,27] apply target-field method to design the biplanar shim coils. An alternative is the passive shimming technique[28,29] using passive ferromagnetic piece configuration to produce different spherical harmonics, whose complexity increases with harmonic order. In addition, the magnetic moment of a passive iron piece is uni-orientational, its magnitude depends on the strength of the local magnetic field

*Project supported by the National Natural Science Foundation of China (Grant No. 60871001).

†Corresponding author. E-mail: dlzu@pku.edu.cn

‡Present address: Microsoft Advanced Technology Centre, 3F, Building 5,555 Dong Chuan Road, Shanghai 200241, China

© 2010 Chinese Physical Society and IOP Publishing Ltd

unless saturated, and the passive iron or steel pieces have magnetic coupling between them and interfere with each other. Despite the passive ferromagnetic shimming approach gives rise to technological difficulties, especially compensating high ordered harmonics, passive shimming is still the preferred method due to its advantages that no power is required and passive ferromagnetic pieces are less expensive than active current shimming coils.

Three-dimensional and two dimensional finite element analysis (FEA) techniques have also been used for preliminary mechanical shimming.[30,31] However, the application of FEA has encountered its bottle-neck because its precision is inadequate to meet the stringent technical demand in MRI. Though mechanical shimming has the merit that requires no extra power and low implementation cost, it has generally been empirical.

The aim of this paper is to extend Dorri and Vermilyea's method[7] from cylindrical SC magnet to biplanar-pole permanent one and substituting passive ferromagnetic pieces (such as iron pieces) with active ones, such as NdFeB pieces. However, the active ferromagnetic (AFM) shimming method presented here is a sort of linear mapping[32] that directly links magnetic field to the sources without correspondence to spherical harmonics. The reason why AFM material not iron is used in this kind of shimming is because AFM pieces have invariable magnetic dipole moment.

2. Methods

Figure 1 shows a typical C-magnet with a pair of opposing parallel shimming boards nearby the gradient coil sets attached to each pole face. Hole locations containing AFM pieces are evenly positioned on the shimming boards as shown in Figs. 2(a) and 2(c). The thickness of a shimming board base of course is larger than the depth of hole which determines the maximal thickness of a magnetic dipole in it. These AFM pieces with its saturation magnetisation ($M_0 = B_r/\mu_0$) are fixed in holes of the shimming boards and the magnetic field of interest is created in the space between them. Each shimming board has finite thickness, say 10 mm at most, so the holes in it have smaller depth, say 8 mm at most. In addition each shimming board is covered with a thin plastic plate to pressurise these pieces in it. This kind of construction provides the ease of fabrication and assembly of AFM pieces with required thickness. The shimming process begins by measuring the magnetic flux density at all the sampling points over the imaging volume. The distribution of ΔB, which is the deviation of the flux density from its expected value, can be obtained by measurement. The object of shimming is to find reasonable locations and thickness of AFM pieces on the shimming boards so that ΔB is eliminated, thereby to better reduce three-dimensional magnetic field inhomogeneity.

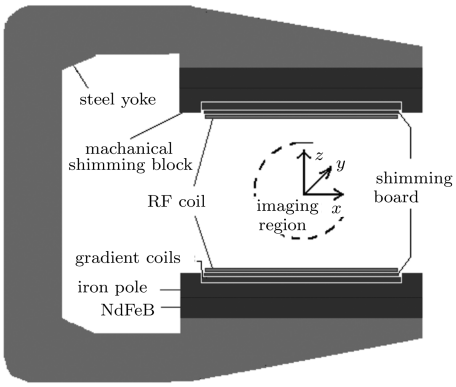
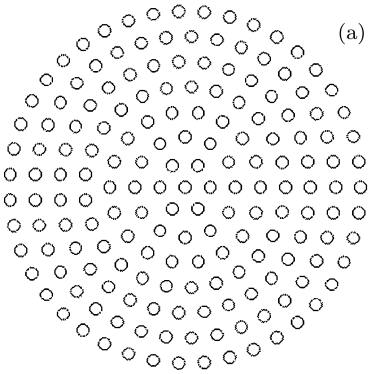
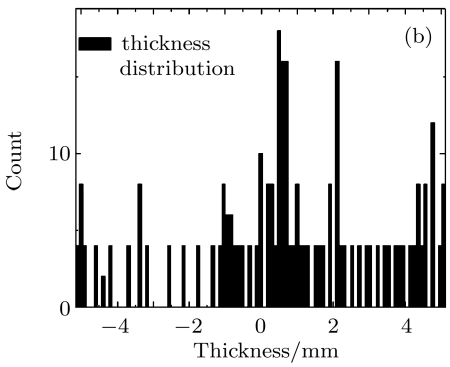


Fig. 1. The 'C'-type permanent magnet and calculation model.





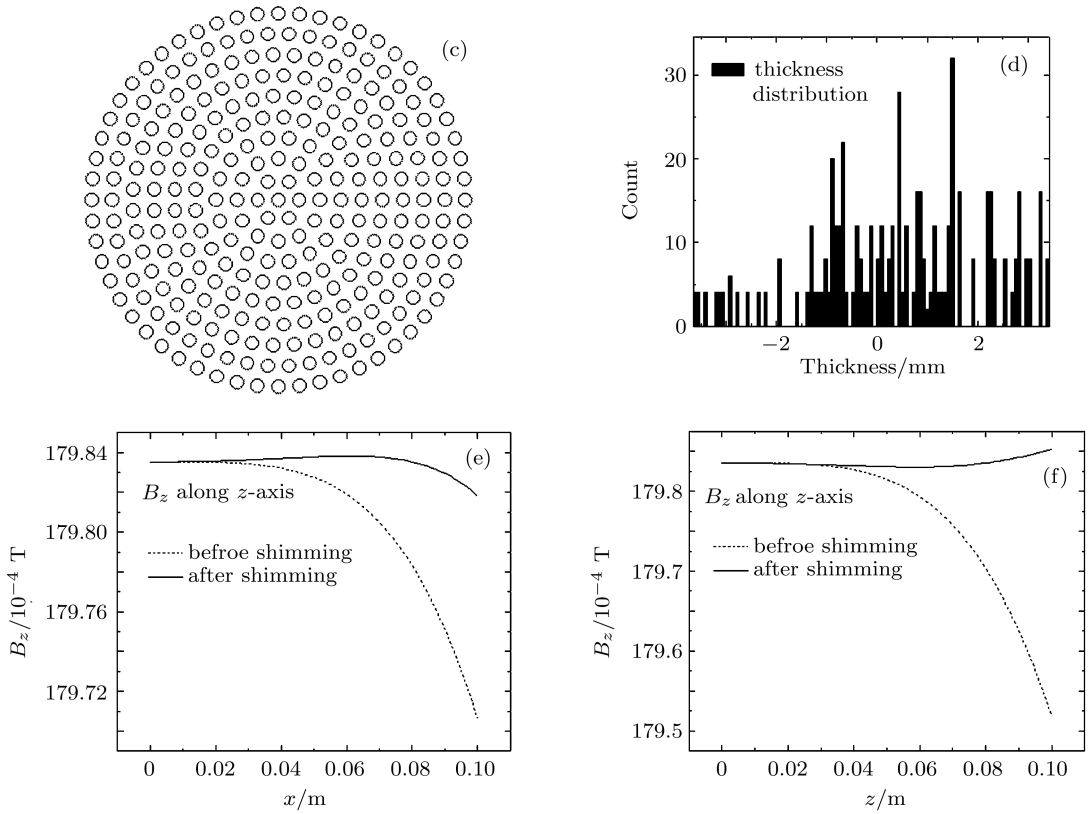


Fig. 2. Comparison of the dependency relation of the maximal thickness of dipole versus the number of hole locations under the same shimming effect. (a) The configuration of holes for AFM pieces positioned on each shimming board, the total number of hole is 346; (b) the statistical thickness distribution of magnetic dipoles which is needed to be positioned on the two shimming boards, the maximal thickness is 5.1 mm; (c) the configuration of holes for AFM pieces positioned on each shimming board, the total number of hole is 558; (d) the statistical thickness distribution of magnetic dipoles which is needed to be positioned on the two shimming boards, the maximal thickness is 3.6 mm; (e) field distribution along x-axis before (dashed) and after (solid) shimming; (f) field distribution along z-axis before (dashed) and after (solid) shimming.

In this method the thickness and orientation of the AFM pieces in the shimming boards is the designing variable to be determined. The magnetic moment of the AFM pieces at each location may be positive or negative. Therefore a good algorithm and an optimisation computer code are needed.

3. Theory

According to Maxwell electromagnetic theory,[33] the magnetic induction field generated by a point magnetic dipole is

$$\boldsymbol{B} = \frac{\mu_0}{4\pi}\frac{3(\boldsymbol{\mu}\cdot\boldsymbol{r})\boldsymbol{r} - \boldsymbol{\mu}\, r^2}{r^5}, \tag{1}$$

where $\boldsymbol{\mu}$ is the magnetic moment of a magnetic dipole and μ_0 is the vacuum magnetic permeability. In the case of AFM shimming, the AFM pieces are circular or square. The AFM pieces piled at each hole location in the shimming boards can be deemed as magnetic dipoles orientating to $\pm$ z-axis while the shimming boards lie at $z' = \pm z_0$ respectively. In practice the AFM pieces should be inserted into the predetermined holes of each shimming board. We only need to concern the B_z-component within the central sphere volume generated by these dipoles because $\boldsymbol{B}$ field is determined to be homogeneous if one of its three components is homogeneous. Suppose $\boldsymbol{r}_i$ represents the coordinate of the ith measured field point; $\boldsymbol{r}'_j$ represents the coordinate of the jth source point. The magnetic induction field at $\boldsymbol{r}_i$ generated by the jth magnetic dipole can be written as

$$\begin{aligned} & B_z^j(\boldsymbol{r}_i) \\ &= \frac{\mu_0\mu_j}{4\pi}\frac{2(Z_i - Z'_0)^2 - (X_i - X'_j)^2 - (Y_i - Y'_j)^2}{\left|\boldsymbol{r}_i - \boldsymbol{r}'_j\right|^5}. \end{aligned} \tag{2}$$

Accounting for the mirror images of the magnetic dipole with respect to the iron pole-face of the magnet,

Eq. (2) should be substituted as

$$B_z^j(\boldsymbol{r}_i) = \frac{\mu_0\mu_j}{4\pi} \times \sum_{k=0}^{\infty} \frac{2(Z_i - Z'_k)^2 - (X_i - X'_j)^2 - (Y_i - Y'_j)^2}{\left|\boldsymbol{r}_i - \boldsymbol{r}'_{jk}\right|^5}. \tag{3}$$

Let M express the m dimensional serial of magnetic dipoles, B the n dimensional serial of compensation induction field. The linear relationship is expressed as

$$B = \boldsymbol{A}M, \tag{4}$$

where $\boldsymbol{A}$ is the $n \times m$ dimensional transformation matrix. By matrix method,[13] this problem can be solved directly by inversing the matrix $\boldsymbol{A}$ if n equals m. However, M calculated in this way is distinctly definite and may not be controlled. In order to overcome this difficulty, we developed a method that minimises the sum of squared magnetic moment. The dimension m should be greater than n in order to give space for confinement. The confinement can be written in matrix form

$$\text{minimize} \quad \boldsymbol{F} = M^{\mathrm{T}}M. \tag{5}$$

Using Lagrange's method of undetermined multipliers, we construct the target function as

$$G = M^{\mathrm{T}}M - 2\boldsymbol{\lambda}^{\mathrm{T}}(\boldsymbol{A}M - B), \tag{6}$$

where $\boldsymbol{\lambda}$ represents Lagrange's multiplier vector. Applying $\partial G/\partial M_i = 0$ one can get

$$\boldsymbol{M} = \boldsymbol{A}^{\mathrm{T}}\boldsymbol{\lambda}. \tag{7}$$

Inserting vector $\boldsymbol{M}$ into original field equation, one can derive

$$B = \boldsymbol{A}\boldsymbol{M} = \boldsymbol{A}\boldsymbol{A}^{\mathrm{T}}\boldsymbol{\lambda}. \tag{8}$$

Here $\boldsymbol{A}\boldsymbol{A}^{\mathrm{T}}$ is an $n \times n$ dimensional squared matrix. Assuming the existence of its inverse matrix, we can obtain vector $\boldsymbol{\lambda}$ as

$$\boldsymbol{\lambda} = (\boldsymbol{A}\boldsymbol{A}^{\mathrm{T}})^{-1}B. \tag{9}$$

The optimized magnetic dipole moment vector is calculated by the equation

$$\boldsymbol{M} = \boldsymbol{A}^{\mathrm{T}}\boldsymbol{\lambda} = \boldsymbol{A}^{\mathrm{T}}(\boldsymbol{A}\boldsymbol{A}^{\mathrm{T}})^{-1}B = \boldsymbol{A}_v B. \tag{10}$$

After that the optimal thickness of the jth dipole consists of AFM pieces can be determined if the remanence of the ferromagnetic material is known,

$$t_j = \frac{\mu_0}{B_{\mathrm{r}}S}M_j, \tag{11}$$

where B_r represents the remanence and S the area of the AFM pieces. Note that there is only one inverse operation of an $n \times n$ dimensional matrix in the overall process. Typically n is restricted to at most several tens for the convenience of field sampling. So the most time consuming inversion operation in this algorism will not bring inefficiency and inaccuracy. Also note that for permanent MRI magnets manufactured in batches with same parameters, the inverse transformation matrix $\boldsymbol{A}_v = \boldsymbol{A}^{\mathrm{T}}(\boldsymbol{A}\boldsymbol{A}^{\mathrm{T}})^{-1}$ can be determined in advance because it only involves geometric parameters. Only a single matrix multiplication is necessary after routine field sampling for individual MRI magnet.

4. Results

First of all a numerical inspection is presented to test the approach. Consider the quasi-homogeneous magnetic field generated by Helmholtz coil pair instead of the permanent magnet for the sake that its magnetic field can be analytically determined. A series of field points are chosen and the numerical values of magnetic field are used as input to the shimming method. The homogeneity of compensated field is investigated to demonstrate the effectiveness of the method. Table 1 shows some geometric parameters of the investigated Helmholtz coils and the shimming boards, and corresponding results.

Table 1. Parameters of the Helmholtz coil pair.

radius of main coils/m	0.5
distance between main coils/m	0.5
SC current supposed/A	10000
central magnetic field/T	179.8353×10^{-4}
radius of shimming boards/m	0.3
distance between up and low boards/m	0.5
radius of each NdFeB piece/cm	1
radius of target imaging region/m	0.10
configuration of sampling	3×3×3
lattice constant of sampling points/m	0.08
number of sampling points n	27
homogeneity before shimming	1.76×10^{-4}*
homogeneity after shimming	1.17×10^{-4}*
total number of shimmed points (case I)	346
maximal thickness of magnetic dipole/mm	5.1
total number of shimmed points (case II)	558
maximal thickness of magnetic dipole/mm	3.6

*observed on z-axis.

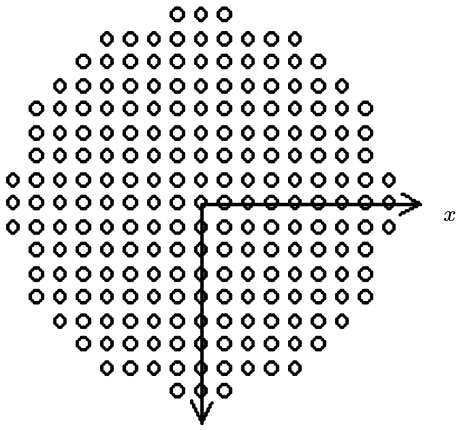
Sampled field points are chosen as equidistant cubic lattices. For comparison of the dependency relationship of the maximal dipole thickness to the number of shimming locations, we investigate two cases. In case I, the configuration of hole locations on both shimming boards is shown in Fig. 2(a), the total number of shimmed points on the shimming boards is 346. Among them only 8 points have the maximal dipole thickness of 5.1 mm. Figure 2(b) shows the statistics of thickness distribution for those determined dipoles which are used in the shimming procedure and a negative sign means that it is set up inversely. In case II, the total number of shimmed points on the shimming boards is 558 (refer to Fig. 2(c)). Among which only 4 points have the maximal dipole thickness of 3.6 mm as shown in Fig. 2(d). In both cases no apex exists at any points on the shimming boards, and the field homogeneity is improved over one and half order of magnitude from 1.76×10^{-4} to 1.17×10^{-4} as is indicated in the last two rows in Table 1. Figures 2(e) and 2(f) show the field distributions before and after shimming for the larger region (20 cm diameter sphere volume (DSV)). Corresponding to the smaller region (13.6 DSV) where the homogeneity is improved from 2.35×10^{-4} to 0.15×10^{-4}. The numerical calculation for one time takes less than 1 second on general personal computers.

For the same coil pair, same target homogeneity requirement, when the number of shimmed points increases (refer to Table 1 and Fig. 2) the maximal thickness of dipole will decrease. Because the gap space between opposing parallel pole faces of the magnet is expensive, increasing the number of hole location in the shimming boards resulting in decreasing the thickness of the shimming boards is of practical significance.

In order to further testify the validity of the method we implement experiments on a permanent magnet with bi-planar poles. The diameter of the magnetic pole surface is eighteen centimeters, the gap between two pole surfaces is eight centimeters. The x-, y-, z-gradient coils lie between the pole surface and the shimming board. For the imaging region of a 30 mm DSV, we have measured these field values at 29 points using a nuclear magnetic resonance (NMR) magnetometer (MetroLab PT 2025 Teslameter). We table data for the measure results as shown in Table 2. The homogeneity of the field measured is peak-to peak 56.0×10^{-5}. For clarity we table the shimming parameters in Table 3. The coordinates of hole locations for AFM pieces in the upper board and the lower board are shown in Figs. 3(a) and 3(c) respectively. The thickness data of magnetic dipole at each hole location where AFM pieces should be inserted is determined from the shimming calculation. For the upper and the lower shimming boards they are displayed on the screen of computer as shown in Fig. 3(b) and 3(d) respectively. The symbol '_' at a hole location means no AFM piece to be put in, i.e. the hole remains empty. The positive (+) or negative (–) sign before each non-zero number at each hole location indicates the orientation of the magnetic moment in it. Here both positive sign for the lower board and the negative sign for the upper board mean that the orientations of the magnetisation of these AFM pieces are all parallel to the z-axis. The homogeneity of the field before shimming is 56.0×10^{-5} (peak-to-peak), whereas after the first time of shimming the field homogeneity calculated is improved to 4.3×10^{-5}.

Table 2. The data measured before shimming.

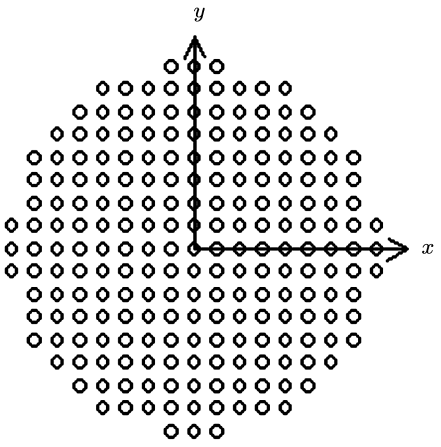
x	y	z	B_z
0	0	15	2923.794
13	0	7.5	2923.621
9.2	9.2	7.5	2923.592
0	13	7.5	2923.599
–9.2	9.2	7.5	2923.581
–13	0	7.5	2923.623
–9.2	–9.2	7.5	2923.741
0	–13	7.5	2923.833
9.2	–9.2	7.5	2923.806
0	0	7.5	2923.669
15	0	0	2923.619
10.6	10.6	0	2923.617
0	15	0	2923.656
–10.6	10.6	0	2923.633
–15	0	0	2923.629
–10.6	–10.6	0	2923.729
0	–15	0	2923.828
10.6	–10.6	0	2923.777
0	0	0	2923.574
13	0	–7.5	2923.092
9.2	9.2	–7.5	2923.164
0	13	–7.5	2923.270
–9.2	9.2	–7.5	2923.248
–13	0	–7.5	2923.183
–9.2	–9.2	–7.5	2923.200
0	–13	–7.5	2923.221
9.2	–9.2	–7.5	2923.148
0	0	–7.5	2923.601
0	0	–15	2924.731



(a)

y\x	-8	-7	-6	-5	-4	-3	-2	-1	0	1	2	3	4	5	6	7	8
-8								_	_	_							
-7					_	_	_	_	_	_	_	_	_				
-6				_	_	_	_	_	_	_	_	_	_	_			
-5			_	_	_	_	_	_	_	_	_	_	_	_	_		
-4		_	_	_	_	_	_	_	_	_	_	_	_	_	_	_	
-3		_	_	_	_	_	_	_	_	_	-0.08	_	_	_	_	_	
-2		_	_	_	_	_	_	-0.21	-0.12	_	-0.06	_	_	_	-2.47	-3.15	
-1	-4.00	-0.13	_	_	_	_	-0.03	-0.13	-0.04	-0.22	-0.05	_	_	_	-3.70	-4.00	-3.90
0	-4.00	_	_	_	_	_	-0.19	-0.07	-0.09	-0.21	-0.16	_	_	-2.22	-4.00	-4.00	-4.00
1	-4.00	-4.00	-3.36	_	_	_	-0.27	-0.11	_	-0.22	-0.08	_	_	_	-4.00	-4.00	-4.00
2		-4.00	-0.10	_	_	_	_	-0.15	-0.25	-0.10	-0.06	_	_	-0.52	-2.20	-3.56	
3		-4.00	_	_	_	_	_	_	_	-0.16	-0.14	_	_	_	_	_	
4		-4.00	_	_	_	_	_	_	_	_	_	_	_	_	_	_	
5			-0.01	_	_	_	_	_	_	_	_	_	_	_	_		
6				_	_	_	_	_	_	_	_	_	_	_			
7					_	_	_	_	_	_	_	_	_				
8								_	_	_							

(b)



(c)

y\x	-8	-7	-6	-5	-4	-3	-2	-1	0	1	2	3	4	5	6	7	8
8								_	_	_							
7					_	_	_	_	_	_	_	_	_				
6				_	_	_	_	_	_	_	_	_	_	_			
5			_	_	_	_	_	_	_	_	_	_	_	_	_		
4		+2.76	_	_	_	_	_	_	_	_	_	_	_	_	_	_	
3		+3.28	_	_	_	_	_	_	_	_	_	_	_	_	_	+0.24	
2		+3.45	_	_	_	_	_	+0.22	+0.22	+0.29	_	_	_	_	_	+0.90	
1	+4.00	+4.00	+1.56	_	_	_	+0.33	+0.13	_	+0.15	+0.12	_	_	_	+4.00	+4.00	+4.00
0	+3.41	_	_	_	_	_	+0.21	+0.02	_	+0.22	+0.18	_	_	_	+4.00	+4.00	+4.00
-1	+4.00	+0.11	_	_	_	_	+0.30	+0.17	+0.01	+0.24	+0.01	_	_	_	+4.00	+4.00	+1.01
-2		+0.70	_	_	_	_	_	+0.20	+0.22	+0.25	_	_	_	_	+1.41	+1.64	
-3		_	_	_	_	_	_	_	_	_	+0.02	+0.01	_	_	_	_	
-4		+0.02	_	_	_	_	_	_	_	_	_	_	_	_	_	_	
-5			_	_	_	_	_	_	_	_	_	_	_	_	_		
-6				_	_	_	_	_	_	_	_	_	_	_			
-7					_	_	_	_	_	_	_	_	_				
-8								_	_	_							

(d)

Fig. 3. The experimental results on a permanent magnet: (a) the coordinate layout of the hole locations for AFM pieces; (b) the distribution of the thickness (in mm) of dipole corresponding to each location in the upper shimming board; (c) the coordinate layout of the hole locations for AFM pieces; (d) the distribution of the thickness of dipole corresponding to each location in the lower shimming board.

It is impossible to make the piece thickness arbitrarily thin because of the brittleness and briability of the NdFeB material. So if in a hole the AFM piece thickness is smaller than 0.5 mm, the AFM piece should be substituted as one with a smaller radius and a larger thickness. It works as long as the dipolar moment of the AFM piece equal to the value determined by shimming calculation. We prepare two sets of AFM pieces with diameter 6 mm and 2 mm, thickness of 0.5, 0.6, 0.7, 0.8, 0.9, 1.0, 1.1, 1.2, 2.0 mm. For these nonempty hole locations as shown in Figs. 3(b) and 3(d), the thickness values determined by shimming calculation can be approached as exactly as possible through overlapping a number of AFM pieces with suitable thickness and diameter.

After inserting AFM pieces into the determined holes of the shimming boards and fixing these AFM pieces having right thickness in each hole, these two shimming boards are restored to the magnet. Then we repeat the shimming process identical to the last time as further correction. We measure the magnet field again like last time. On the one hand we check the effect of the first time of shimming process, on the other hand this is the beginning of the secondary shimming process. From second shimming on, we adjust the number of AFM pieces in hole determined by second shimming calculation so that the homogeneity is improved more. Specifically, after the first time of shimming the field homogeneity measured is improved to better than 5.0×10^{-5} or so. After the iteration

of the second shimming, the field homogeneity is not difficult to reach better than 2.0×10^{-5} as a specification of magnet. Otherwise repeat shimming until the homogeneity measured is 2.0×10^{-5} or lower than 2.0×10^{-5}. Generally, a tertiary shimming process is not needed. In principle better homogeneity is possible but not meaningful because the field shift with temperature within $\pm 1.0 \times 10^{-5}$ even though under the condition of temperature controlling magnet. A representative image obtained with this magnet for MRI teaching Lab is shown in Fig. 4.

Table 3. The shimming parameters for a practical magnet.

gap between two pole surfaces/cm	8.0
radius of the area containing AFM piece/cm	8.5
distance between two shimming boards/cm	5.5
distance between hole locations on shimming boards/cm	1.0
radius of each nominal AFM pieces/mm	3
maximal thickness of magnetic dipole/mm	4
remanence of NdFeB pieces ($B_{\rm r}$)/T	1.2
total numbers of hole locations on two boards	426
strength of the central field/T	0.2923574
point numbers of measuring field within 30 mm DSV	29
homogeneity of the field before shimming	5.60×10^{-4}
homogeneity of field after first time of shimming	0.43×10^{-4}

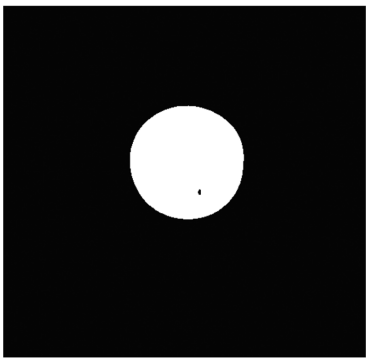


Fig. 4. The SE images of water tube.

5. Discussion

In order to acquire credible data of magnetic field, scanning the probe over the 29 field point locations has soon the possibility to get rid of the effect of temperature shift of the permanent magnet. The sampling points need to be accurately positioned and the instrument measuring the magnet field should be NMR teslameter. Generally a Hall teslameter is not fit, especially in the case of finely shimming. Accounting for the demagnetisation effect in the permanent material, the AFM pieces must be magnetised in an external field as a few times high as its $B_{\rm r}$ to obtain homogeneous and consistent M_0.

Because the operation of inserting the AFM pieces in each hole of the shimming boards is carried out outside the magnet, firstly we should not confuse the upper and the lower shimming board, secondly we should not mistake the polarity of each magnetic dipole, especially we should need to pay attention to the magnetic dipole direction in the upper shimming board. The upward dipoles in the magnet become downward when removing the upper shimming board from magnet and laying it on the floor.

For the case that hole size is larger than AFM piece size, it is necessary to hold the AFM piece in the central hole of a plastic chip which fits the hole in the shimming board. In addition, generally speaking the calculated results of the dipole thickness is not unique, depending on the layout of hole location in the shimming boards. According to the target homogeneity requirement the user can choose a most convenient scheme. Finally, as input to the shimming method, the number of sampling point at best does not beyond 100, otherwise the accuracy of calculated results is not sure or no calculated results given.

6. Conclusions

A complete analytical designing methodology for AFM shimming of C-shaped permanent MRI magnet

has been formulated and presented. This approach is adaptive to not only the initial rough shimming procedure but the final refined one too as long as sufficient locations are available in both shimming boards. Both the simulation and experimented results prove that this technique is feasible without a spatial harmonics consideration. Moreover the method is proved to be valid and efficient. It will significantly curtail the shimming phase of MRI apparatus. Recently the method presented is tryout in MRI magnet manufactory.

References

[1] Jin J M 1999 *Electromagnetic Analysis and Design in Magnetic Resonance Imaging* (Boca Raton, Fla.: CRC Press)

[2] Haacke E M, Brown R W, Thompson M R and Venkatesan R 1999 *Magnetic Resonance Imaging, Physical Principles and Sequence Design* (New York: Wiley)

[3] Zu D L 2004 *Magnetic Resonance Imaging* (Beijing: Higher Education Press) (in Chinese)

[4] Hoult D I and Lee D 1985 *Rev. Sci. Instrum.* **56** 131

[5] Bobrov E S, Pillsburg K D, Punchard W F B, Schwall R E, Segal M R, Williams J E and Neuringer I J 1987 *IEEE Trans. Magn.* **23** 1303

[6] Williams J E C 1984 *IEEE Trans. Nucl. Sci.* **31** 994

[7] Dorri B and Vermilyea M E 1993 *IEEE Trans. Appl. Supercond.* **3** 254

[8] Belov A, Bushuev V, Emelianov M, Eregin V, Severgin Yu, Sytchevski S and Vasiliev V 1995 *IEEE Trans. Appl. Supercond.* **5** 679

[9] Vermilyea M E (US Patent) 4771244 [1988-09-13]

[10] Dorri B and Vermilyea M E (US Patent) 5045794 [1991-09-03]

[11] Dorri B (US Patent) 5677854 [1997-10-14]

[12] Roméo F and Hoult D I 1984 *Magn. Reson. Med.* **1** 44

[13] Hoult D I and Deslauriers R 1994 *J. Magn. Reson. Ser.* A **108** 9

[14] Forbes L K and Crozier S 2001 *Med. Phys.* **28** 1644

[15] Turner R 1986 *J. Phys.* D: *Appl. Phys.* **19** 147

[16] Forbes L K and Crozier S 2001 *J. Phys.* D: *Appl. Phys.* **34** 3447

[17] Forbes L K and Crozier S 2002 *J. Phys.* D: *Appl. Phys.***35** 839

[18] Forbes L K and Crozier S 2003 *J. Phys.* D: *Appl. Phys.* **36** 68

[19] Brideson M A, Forbes L K and Crozier S 2002 *Concepts Magn. Reson.* **14** 9

[20] Liu W T, Zu D L and Tang X 2010 *Chin. Phys.* B **19** 018701

[21] Abele M 1993 *Structures of Permanent Magnets* (New York: Jhon Wiley and Sons)

[22] Xia P C 2000 *Structures of Permanent Magnets* (Beijing: BGD Press) (in Chinese)

[23] Abele M, Rusinek H and Bertora F 1992 *IEEE Trans. Magn.* **28** 931

[24] Anderson W A 1961 *Rev. Sci. Instrum.* **32** 241

[25] Coley M J E 1958 *Rev. Sci. Instrum.* **29** 313

[26] Forbes L K, Brideson M A and Crozier S 2005 *IEEE Trans. Magn.* **41** 2134

[27] Forbes L K and Crozier S 2004 *IEEE Trans. Magn.* **40** 1929

[28] Battocletti J H, Kamal H A, Myers T J and Knox T A 1993 *IEEE Trans. Magn.* **29** 2139

[29] Zhang Y L, Xie D X and Xia P C 2003 *Proc. Sixth ICEMS* **2** Beijing, Nov. 9–11, 2003

[30] Battocletti J H and Myers T J 1989 *IEEE Trans. Magn.* **25** 3910

[31] Battocletti J H and Knox T A 1985 *IEEE Trans. Magn.* **21** 1874

[32] Hong L and Zu D 2007 *Piers on Line* **3** 859

[33] Jackson J D 1976 *Classical Electrodynamics* (New York: Wiley)